Characterization of Systematic Process Variation in a Silicon Photonic Platform

Nicholas Boynton,[1,2] Andrew Pomerene,[1] Andrew Starbuck[1], Anthony Lentine[1] and Christopher T. DeRose[1]

[1] *Sandia National Laboratories, P. O. Box 5800, Albuquerque, NM 87185, USA*

[2] *Department of Electrical & Computer Engineering, University of New Mexico, Albuquerque, NM 87131, USA*

Abstract: We present a quantitative analysis of the correlation of resonant wavelength variation with process variables, and find that 50% of the resonant wavelength variation for microrings is due to systematic process conditions. We also discuss the improvement of device uniformity by mitigating these systematic variations.

Introduction

Silicon photonics is widely believed to be an enabling technology for next generation large scale optical interconnects. In particular, microdisk and microring resonator devices have been shown to provide compact, low energy, wavelength division multiplexed (WDM) optical communications [1]. However, the device physics which leads to low energy modulation and switching in micro-resonators comes at the cost of extreme sensitivity to process variation. In recent years the topic of uniformity and process variation of silicon micro-resonators has been a topic of research interest [2-4]. In this paper we present an analysis of the statistical distribution of resonant frequencies of ~6 μm diameter microring resonators fabricated in Sandia National Laboratories Mesa foundry. In our analysis we find that 50% of the resonant wavelength variation is due to systematic and technical noise contributions. We discuss both the mitigation of the systematic variation and a path towards improved device uniformity.

Experiment and Results

In order to characterize the variation in resonant frequency in Sandia's 150 mm wafer, 248 nm lithography silicon photonics process a mask set was designed which consists of five cascaded microring resonators. A dark filed micrograph of a group of fabricated microring resonators is shown in Fig. 1 (a). The five microring resonators have equal waveguide width and varying outer diameters and coupling gaps (6.00, 6.03, 6.06, 6.09, 6.12 μm and 360, 340, 320, 300, 280 nm, respectively). A second set group of five identical ring resonators were positioned 15 μm away, which were not used in this experiment as short range disorder has been previously shown to be low [3]. These two sets of ring resonators form a unit cell which is repeated every 1000 μm laterally and 400 μm vertically. A total of 1680 unit cells are on each die with 16 complete die per wafer for a total of 268,800 microrings per wafer. In this study, we present statistics of data measured from 3360 of those microrings across a 150 mm wafer. There is also another strip waveguide used for alignment and normalization of resonator spectrum to the loss of the fiber grating couplers. Wafers were fabricated with a passive silicon photonic process flow consisting of an 80 nm partial silicon etch, a full thickness silicon (~230 nm) etch, and cladding in 2.4 μm thick high density plasma (HDP) oxide.

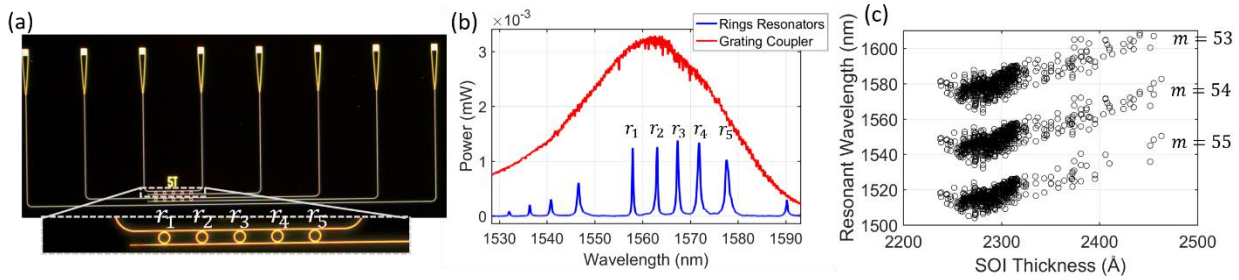

Figure 1 (a) Dark field microscope image of a unit cell. (b) Typical transmission spectrum through grating couplers and drop port of a unit cell. (c) Resonant wavelength of 6 μm diameter ring across the wafer plotted vs. final silicon device layer.

The resonant wavelength of a microring resonator, is given by $\lambda_{res} = (2\pi r/m) \cdot n_{eff}(t, w, \lambda)$ where, r is the radius of the microring, m is the azimuthal mode number, n_{eff} is the effective index of the propagating mode, t is the waveguide thickness, w is the waveguide width and λ is the wavelength. Thus, it is clear that perturbations in the resonator thickness, width and radius are the variables which most strongly influence the resonant wavelength. The sensitivity to geometric variation of the 6.00 μm diameter ring resonator (r_1 in Fig. 1(a)) is modeled using FDTD simulation. From the results of these simulations, a first order model of resonant wavelength as a function of the ring resonator waveguide cross-sectional dimensions is developed, which is seen in Eq. 1,

$$\lambda_{res} = \lambda_0 + \alpha(t - t_0) + \beta(w - w_0) \quad (1)$$

where λ_{res}, t, and w are the wavelength, waveguide thickness and widths respectively, α and β are the thickness and width dependencies. In Eq. 1, λ_0 is 1550 nm, w_0 is 400 nm and t_0 is 238 nm. The thickness dependency α is found to be 1.25 nm shift in resonance per nm change in silicon-on-insulator (SOI) thickness, and the width dependency β is found to be 1.08 nm shift in resonance per nm change in waveguide width.

Prior to fabrication, the SOI layer thickness was measured using spectroscopic ellipsometry. A contour map of the wafer thickness can be seen in Fig. 2 (a). From this contour plot it is clear that the silicon device layer thickness varies systematically with a tilted radial dependence which has a sharp gradient at the edge of the wafer, likely due to a combination of bonding/cleaving and CMP in the manufacture of the wafer. The standard deviation in wafer thickness, σ_t, is measured to be 3.9 nm. The variation in lithographic feature size post-etch were measured with a CD-SEM. A contour plot of the wafer waveguide width post-etch is shown in Fig. 2 (b). We find the distribution of waveguide width across the wafer is not uniform, rather it has a radial dependence, possibly due to variation in the temperature of the hotplate used in the post exposure bake. We find that the post-etch waveguide width has a standard deviation, σ_w, of 5.2 nm. A contour map of the resonant wavelength measured across the wafer is shown in Fig. 2 (c), which we find to have a standard deviation, σ_λ, of 6.85 nm

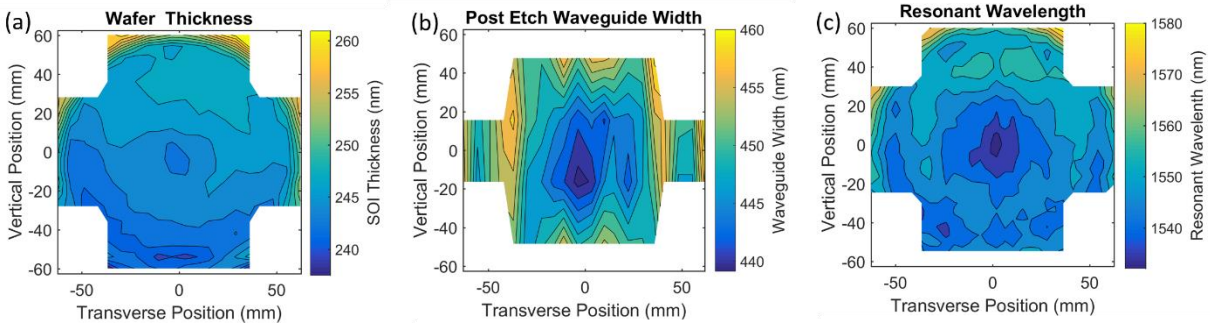

Figure 2(a) Contour plot of measured silicon device layer thickness. (b) Contour plot of post-etch waveguide width. (c) Contour plot of resonant wavelength of 6 μm diameter ring.

Measurement of resonant wavelength across the wafer was done in a Cascade Microtech Summit probe station. Transverse electric (TE) polarized light from an Agilent tunable laser, swept from 1495 – 1610 nm, is coupled into and out of the device through a 127 μm pitch fiber array angled at 8°. The transmission spectrum for each unit cell was measured at a spacing of 4 mm for all 16 full die on the 150 mm wafer. Alignment of the fiber array to the device, stepping of the wafer, and data collection was automated. A typical transmission spectrum of the fiber grating coupler and ring resonators is shown in Fig. 1 (b). Spectra from the microring resonators is normalized to the transmission through the grating couplers to flatten the spectrum (Fig. 1 (b)), then resonant wavelength is found by using a noise robust peak finding algorithm. A consistent azimuthal order m of each resonant wavelength is found by only considering those resonances which are clearly grouped as a function of wafer thickness as seen in Fig. 1 (c), which enables the tracking of the resonant wavelength over separations that were larger than one FSR. From FDTD simulations we calculate that the mode number is 54 near 1550 nm.

The degree of correlation between resonant wavelength, thickness and waveguide width is quantified using the linear correlation coefficient, and we find that the resonant wavelength is well correlated with the silicon thickness, waveguide width and radial position, the details of this analysis will be presented. In order to estimate the effect of improvement in processing conditions on resonant wavelength variation the correlation with the random variables is removed. By removing the correlation with both the SOI thickness and positional dependence of lithography, we find the standard deviation of resonant wavelength is reduced to 3.45 nm, an improvement of 50%. SOI uniformity can be improved with several approaches such as coring a 300 mm wafer or using local etching of the silicon device layer, which can reduce the standard deviation of the SOI thickness to 0.9 nm [4]. The positional dependence of the lithography can be removed in practice by improving the temperature uniformity of the post exposure bake.

Conclusions

We present for the first time a quantitative analysis of the correlation of resonant wavelength variation with process variables. We find that the variation in resonant wavelength is due in large part to systematic process conditions. Importantly the sources of technical noise in Sandia's 150 mm wafer, 248 nm lithography process can be mitigated with process refinement, which we predict will lead to a 50% improvement in device uniformity.

This work is supported by the Laboratory Directed Research and Development program at Sandia National Laboratories, a multi-mission laboratory managed and operated by Sandia Corporation, a wholly owned subsidiary of Lockheed Martin Corporation, for the U.S. Department of Energy's National Nuclear Security Administration under contract DE-AC04-94AL85000.

[1] A. L. Lentine, *et al.*, "Silicon Photonics Platform for National Security Applications" Aerospace Conference (2015).

[2]S. K. Selvaraj, et al., "Subnanometer Linewidth Uniformity in Silicon Nanophotonic Waveguide Devices Using CMOS Fabriacation Technology," IEEE JSTQE, vol. 16, pp. 316-324 (2010).

[3] L. Chrostowski, *et al*, "Impact of Fabrication Non-Uniformity on Chip-Scale Silicon Photonic Integrated Circuits," Optical Fiber Communication Conference (OFC), paper Th2A.37 (2014).

[4] S. K. Selvaraja, *et al.,* "SOI thickness uniformity improvement using corrective etching for silicon nano-photonic device" Group IV Photonics (GFP), paper P1.5 (2011).